New mechanism for the dissolution of sparingly soluble minerals*

Ruikang Tang and George H. Nancollas[‡]

Department of Chemistry, Natural Sciences Complex, University at Buffalo, State University of New York, Buffalo, NY 14260, USA

Abstract: A requirement for the determination of the solubility of minerals is to ensure that equilibrium has been reached. Recent constant composition dissolution studies of sparingly soluble calcium phosphates have revealed an interesting and unusual behavior in that the rates decreased, eventually resulting in effective reaction suppression, even though the solutions remained undersaturated. Traditional theories of dissolution assume a volume diffusion-controlled mechanism with reaction continuing until true equilibrium has been reached. The new results for sparingly soluble salts point to the importance not only of particle size on the dissolution rate but also the participation of critical phenomena. Although the crystal size decreases during dissolution, when the reaction is controlled by poly-pitting (the formation and growth of pits), the edge free energy increases at the very first stage of reaction owing to the creation of pits and dissolution steps. The constant composition experimental results demonstrate the development of surface roughness as the dissolution steps are formed, implying an increase of the total edge length during the reaction. This is an exactly analogous mechanism to that of crystal growth, in which the formation of embryos of critical size plays a key role in the overall mechanism. In contrast to crystal growth, dissolution is a process of size reduction, and, when the particle size is sufficiently reduced, critical phenomena become important so that the influence of size must be taken into consideration. It is interesting to recognize that these critical phenomena are readily apparent for sparingly soluble minerals for which the critical conditions are attained much more readily. The results point to the importance of understanding the detailed mechanism of dissolution when attempts are made to measure, experimentally, the solubilities of sparingly soluble minerals.

SOLUBILITY

Although the Ostwald–Freundlich equation expresses the variation of solubility as a function of particle size and interfacial tension [1–3], it is generally accepted that neither the amount of excess solid nor the size of the particles will change the position of the equilibrium, and thermodynamic considerations are applicable in aqueous solutions [4,5]. The solubility of a substance in a given solvent may be expressed in terms of any units that serve to indicate the relative amounts of the components (e.g., g/100g or mol fraction). For sparingly soluble salts, solubilities are always defined by ion activity products, K_s, as eq. 1,

$$K_s = \prod_i a_i^{v_i} \qquad (1)$$

in which a_i and v_i are the activity of ion i and its number in a formula unit of the dissolving phase, respectively. Accordingly, the degree of supersaturation, S, is given by eq. 2,

$$S = \left(\frac{IP}{K_s}\right)^{1/\sum_i v_i}$$ (2)

IP is the ionic activity product, $S > 1$, $S = 1$, and $S < 1$ representing supersaturation, saturation, and undersaturation, respectively. In order to determine the value of solubility, equilibrium should be approached both by crystal growth and by dissolution.

CRYSTALLIZATION AND METASTABLE SUPERSATURATION

It has long been recognized that in practice, precipitation does not occur instantaneously upon the creation of very low supersaturations [6]. There is a metastable zone in which the solution remains stable, and only after a period of time (the "induction period", τ), are new crystals detected. It is also well known that the nucleus size, r, and interfacial energy, γ_{SL}, are involved in the free energy of crystal formation, ΔG, expressed as eq. 3 [6],

$$\Delta G = \frac{4\pi r^3}{3\Omega_V}\Delta g + 4\pi r^2 \gamma_{SL}$$ (3)

In eq. 3, Ω_v is molecular volume and Δg is the change in Gibbs energy per molecule. The dependence of the Gibbs energy on r passes through a maximum, $\partial\Delta G/\partial r = 0$, corresponding to the critical size, r^* and critical Gibbs energy,

$$r^* = \frac{2\gamma_{SL}\Omega_V}{\Delta g}$$ (4)

Equations 3 and 4 imply that crystallization is not spontaneous until the nuclei reach a size, r^*. Previous experimental data have shown that there is a close relationship between solubility and γ_{SL} [7,8]. Higher values of γ_{SL} indicate a greater difficulty in forming a solid–liquid interface, and sparingly soluble salts always have relatively high surface tensions in aqueous solution [4,8]. As a result, it has been found that they have relatively wide metastable supersaturated zones with extended induction times, τ, for homogeneous crystallization. Thus, for hydroxyapatite [$Ca_{10}(PO_4)_6(OH)_2$, HAP], a major inorganic component in hard tissues, at relatively high supersaturation ($S = 18$), τ is greater than 10 h.

UNUSUAL DISSOLUTION AND SOLUBILITY PHENOMENA

It is much more convenient to approach solubility equilibrium through dissolution rather than growth [9–14]. In most kinetic studies, dissolution has been expressed analogously to the surface diffusion control of the crystal growth [6,15,16], implying that the dissolution rate should be constant when the undersaturation is maintained and that dissolution continues until equilibrium is reached. However, it has been found that this simple representation of dissolution is unsatisfactory for many sparingly soluble biominerals. In previous solubility studies, some minerals were found to be resistant to dissolution in undersaturated solutions, and the concept of an intermediate metastable state was introduced [17–21] with solubility related to particle size [20]. Recently, constant composition (CC), a highly reproducible technique for kinetic studies of crystallization and dissolution of sparingly soluble salts, has shown that calcium phosphate dissolution rates decrease markedly with time despite a sustained undersaturation, eventually resulting in effective reaction suppression even though the solutions remained undersaturated [22–25]. For octacalcium phosphate [$Ca_8H_2(PO_4)_6\cdot5H_2O$, OCP] dissolution (Fig. 1), it can be seen that
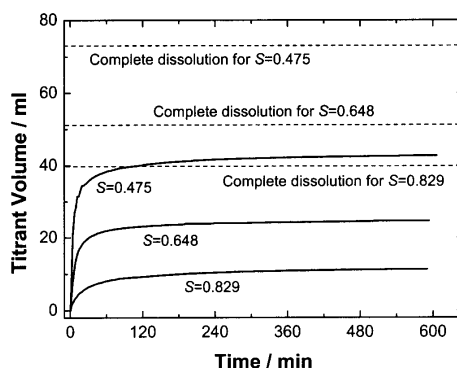
Fig. 1 Plots of titrant volume against time for OCP dissolution at different undersaturations. The rates decrease virtually to zero; dashed lines show the calculated titrant volume for complete crystal dissolution. The percentages of dissolved crystals increased from 30 % at $S = 0.829$ to 55 % at $S = 0.475$.

the reaction was effectively suppressed before all the solid phase had dissolved in the undersaturated solution; only 55 % of the seed crystals underwent dissolution at $S = 0.475$. This percentage further decreased with increase of S, and similar phenomena were observed with other calcium phosphates [23–25].

A NEW UNDERSTANDING OF DISSOLUTION

Recent in situ atomic force microscopic (AFM) and scanning electrochemical microscopic (SECM) studies have revealed that dissolution is initiated by the creation and growth of pits on the crystal surfaces [24,26–29]. Moreover, CC experimental results also indicate a dissolution controlled by poly-pitting [24,25]. When crystallites of brushite ($CaHPO_4 \cdot 2H_2O$, DCPD), were immersed into an undersaturated solution ($S = 0.940$), AFM showed that numerous pits formed immediately on the smooth surfaces, creating reactive dissolution sites. In this first stage of dissolution, the increase of surface roughness resulted in an increase of the solid–liquid interfacial energy. Thus, the surface energy term in eq. 3 is not always negative and the participation of critical phenomena is involved. Only when a pit of critical size is reached does dissolution become spontaneous. Further studies of pit growth rates, $R(r)$, show that their contribution to the dissolution reaction is dependent on their sizes. The relationship is given by eq. 5,

$$R(r) = R_\infty \left(1 - \frac{e^{(1-S) \cdot r^*/r} - 1}{e^{(1-S)} - 1} \right)$$

(5)

in which R_∞ is the rate when the pit is infinitely large. Figure 2 shows a dissolving DCPD surface at $S = 0.940$. After pit creation, subsequent dissolution is accompanied by pit growth, the rate increasing with pit size. These observations are consistent with eq. 5 and with AFM results for calcite growth [30]. When the value of r approaches r^*, the quantity $[e^{(1-S) r^*/r} - 1]/(e^{1-S} - 1)$ is close to 1 and $R(r)$ tends to zero. Thus, although small pits may exist on the surface, they are almost stationary as compared with the larger ones, and they make extremely small contributions to dissolution. These small pits may be removed from the dissolving surface by other, "active", dissolution steps from neighboring large pits. In accordance with eq. 5, small pits that are at a standstill can be regarded as having dimensions close to the critical size (0.2–0.5 μm for DCPD dissolution at $S = 0.940$). Comparing Figs. 2a and b, it can be seen that the pit density decreases during dissolution. Crystal sizes, initially 8–12 μm for DCPD, significantly decrease during dissolution, together with pit sizes.
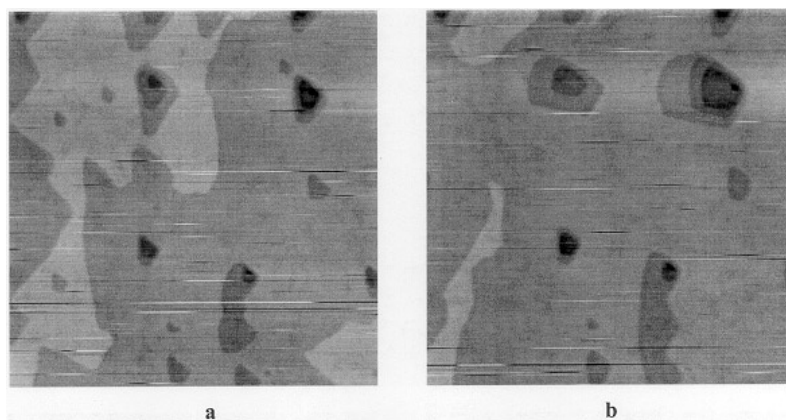
Fig. 2 In situ AFM shows numerous pits (dark areas) on smooth DCPD surfaces when the dissolution is initiated at a low undersaturation of $S = 0.940$. Large pits develop more rapidly than small ones. The interval between (a) and (b) is 7 min, and the image scales are 5×5 μm.
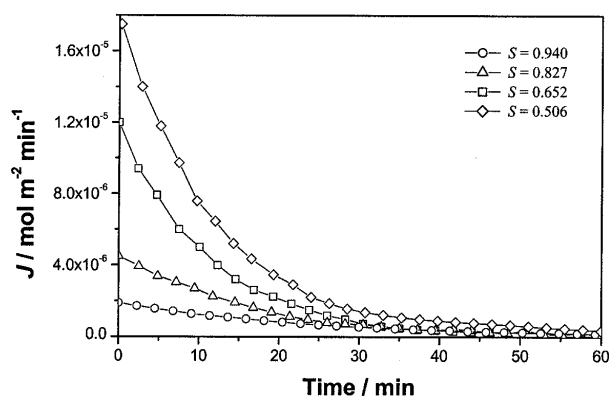

Fig. 3 Plots of dissolution rate (J) against time for DCPD dissolution at different undersaturations.

The decrease in the overall CC dissolution rates to near zero is shown in Fig. 3. However, thermodynamics requires that dissolution cannot stop in an absolute sense in an undersaturated solution. It is suggested that two factors are important; one, the narrowly defined decrease in the density and size of pits, and the other, the surface rearrangement or movement of the pits themselves, disappearing and renucleating during the reaction. Although dissolution almost stops, reaching a pseudo "equilibrium state", the movement of the pits on the surfaces continues extremely slowly, driven by thermodynamic undersaturation requirements. Thus, since the critical condition for reaction suppression cannot be sustained indefinitely, dissolution then resumes until a new critical condition is reached, resulting in the stepwise rate curve at a low undersaturation (close to true equilibrium), shown in Fig. 4 over extended time periods. Although it appears that solubility equilibrium has been reached at each of the plateaux in Fig. 4, the suspension does not reach true thermodynamic equilibrium, and these intermediate plateaux cannot be used for solubility determination.

This unusual behavior is more apparent for the dissolution of sparingly soluble salts, which invariably consist of crystallites of very small sizes and which have high surface tensions resulting in a greater barrier to pit creation. Since the critical size is proportional to γ_{SL} (eq. 4), the relatively high value of r^* and small crystallite size result in critical conditions, which are more readily attained. It can be seen in Fig. 5 that the dissolution rate reduction for large OCP crystallites is much less than that for small
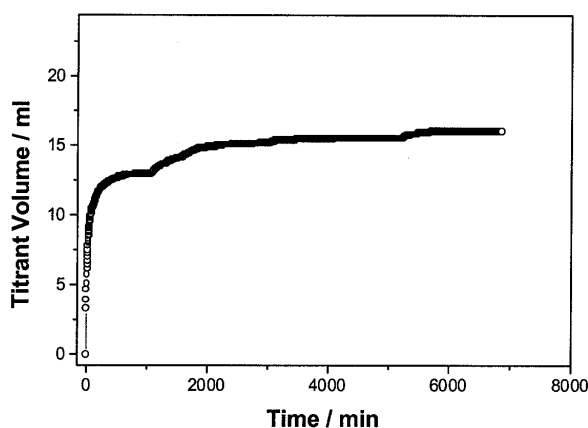
Fig. 4 CC dissolution of "dissolution terminated" OCP crystallites resumes after long time periods ($S = 0.829$), showing characteristic stepwise profiles. The titrant volume corresponding to complete dissolution would be about 40 ml.
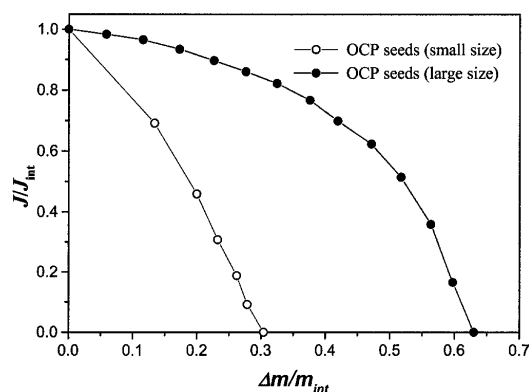

Fig. 5 Plots of J/J_{int} (J, J_{int} are the dissolution rates at time, t and $t = 0$, respectively) against $\Delta m/m_{int}$ (Δm is the dissolved OCP mass and m_{int}, the initial seed mass) for the dissolution of OCP crystals of different sizes. The decrease in J/J_{int} is much greater for the small crystallites.

particles, and more crystallites dissolve before the effective dissolution suppression. It follows that the "abnormal" dissolution behavior for large crystallites is less apparent than that of small particles. In soluble salt systems, r^* values are much smaller (theoretical calculations show values of the order of a few nanometers) and the crystals are usually much larger (on a mm scale). The present stepwise metastable steps in crystallite-liquid equilibrium observed here for sparingly soluble salts have never been observed for more soluble electrolytes.

It can be seen in eq. 4 that the critical condition is also a function of undersaturation; lower undersaturations resulting in greater values of r^*. Critical state phenomena and "abnormal" dissolution behavior then become more noticeable. Assuming that the pit size, r, is proportional to crystallite size, when these are of the same order of magnitude, the extent of dissolution can be related to an equivalent decrease in mean crystallite size. It is known that r^* at lower undersaturation (near $S \sim 1$) is greater than that at higher undersaturation; the change in the term $\{1 - [e^{(1-S)\, r^*/r} - 1]/(e^{1-S} - 1)\}$ is greater, and the decrease of dissolution rate becomes more noticeable. This is clearly shown in Fig. 6 for the dissolution of OCP at different undersaturations.
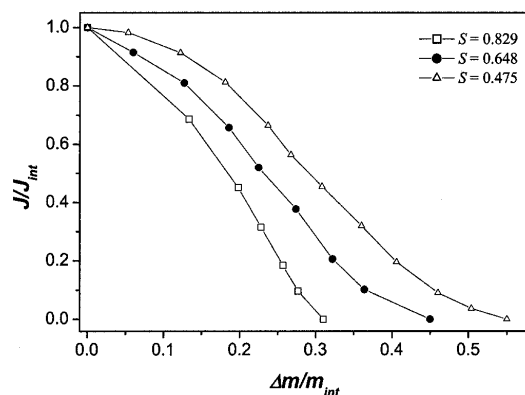
Fig. 6 Plots of J/J_{int} against $\Delta m/m_{int}$ for the dissolution of OCP crystals at different undersaturations. The decrease of J/J_{int} at low undersaturation is greater than that at high undersaturation for the same extent of dissolved mass.

The present results show that although the solubility of a crystal should be independent on its size and surface structure, these two factors may be interrelated owing to dissolution suppression and the existence of metastable undersaturated states. These phenomena are more apparent in the case of sparingly soluble salts such as the biominerals, because of their high surface tensions, large r^* values, and small crystallite sizes, resulting in more readily attained critical conditions. In order to attain "true" equilibrium solubility conditions, for electrolytes in aqueous solutions, large crystallite size and long equilibrium times are recommended. Whenever possible, equilibrium should be approached experimentally from both dissolution and crystal growth.

ACKNOWLEDGMENTS

REFERENCES

1. W. Ostwald. *Z. Phys. Chem.* **34**, 495 (1900).
2. H. Freundlich. *Colloid and Capillary Chemistry*, p. 153, Dutton, New York (1923).
3. W. H. Wollaston. *Phil. Trans.* **103**, 57 (1813).
4. R. Defay and I. Prigogine. *Surface Tension and Adsorption*, Wiley, New York (1966).
5. W. Wu and G. H. Nancollas. *J. Sol. Chem.* **27**, 521 (1998).
6. P. Hartman. *Crystal Growth: An Introduction*, North-Holland, Amsterdam (1975).
7. L. A. Girifalco and R. J. Good. *J. Phys. Chem.* **61**, 904 (1957).
8. W. Wu and G. H. Nancollas. *Adv. Colloid Interface Sci.* **79**, 229 (1999).
9. L. C. Bell, H. Mika, B. J. Kruger. *Arch. Oral Biol.* **23**, 329 (1978).
10. M. S. Tung, N. Eidelman, B. Sieck, W. E. Brown. *J. Res. Natl. Bur. Stand.* **93**, 613 (1988).
11. R. M. H. Verbeeck, H. Steyaer, H. P. Thun, F. Verbeek. *J. Chem. Soc., Faraday Disc.* **76**, 209 (1980).
12. T. M. Gregory, E. C. Moreno, W. E. Brown. *J. Res. Natl. Bur. Stand.* **74A**, 461 (1970).
13. G. H. Nancollas, L. J. Shyu, Y. Yoshikawa, J. P. Barone, D. Svrjcek. *Am. Inst. Chem. Eng.* **78**, 26 (1978).
14. H. McDowell, W. E. Brown, J. R. Sutter. *Inorg. Chem.* **10**, 1683 (1971).

15. A. A. Chernov. *Modern Crystallography III,* Springer Series Solid State, Vol. 36, Springer, Heidelberg (1984).
16. A. A. Chernov. *Prog. Cryst. Growth Charact. Mater.* **26**, 121 (1993).
17. J. Barralet, M. Akao, H. Aoki. *J. Biomed. Mater. Res.* **49**, 176 (2000).
18. F. C. M. Driessens and R. M. H. Verbeeck. *Z. Naturforsch.* **35**, 262 (1980).
19. A. A. Baig, J. L. Fox, Z. Wang, W. I. Higuchi, S. C. Miller, A. M. Barry, R. Otsuka. *Calcif. Tissue Int.* **4**, 329 (1999).
20. A. A. Baig, J. L. Fox, R. A. Young, Z. Wang, J. Hsu, W. I. Higuchi, A. Chhettry, H. Zhuang, M. Otsuka. *Calcif. Tissue Int.* **64**, 437 (1999).
21. H. Zhuang, A. A. Baig, J. L. Fox, Z. R. Wang, S. J. Colby, A. Chhettry, W. I. Higuchi. *J. Colloid Interface Sci.* **222**, 90 (2000).
22. J. Zhang and G. H. Nancollas. *J. Crystal Growth* **123**, 59 (1992).
23. R. Tang and G. H. Nancollas. *J. Crystal Growth* **212**, 261 (2000).
24. R. Tang and G. H. Nancollas. *J. Am. Chem. Soc*. **123**, 5437 (2001).
25. R. Tang, W. Wu, M. Hass, G. H. Nancollas. *Langmuir* **17**, 3480 (2001).
26. C. E. Jones, J. V. Macpherson, P. R. Unwin. *J. Phys. Chem. B.* **104**, 2351 (2000).
27. J. V. Macpherson and P. R. Unwin. *J. Phys. Chem.* **98**, 11764 (1994).
28. J. V. Macpherson, P. R. Unwin, A. C. Hillier, A. J. Bard. *J. Am. Chem. Soc.* **118**, 6445 (1996).
29. P. Risthaus, D. Bosbach, U. Becker, A. Putnis. *Colloids Surf. A* **191**, 201 (2001).
30. H. H. Teng, P. M. Dove, C. A. Orme, J. J. De Yoreo. *Science* **282**, 724 (1998).